

Asymmetric neural tracking of gain and loss magnitude during adolescence

Catherine Insel and Leah H. Somerville

Department of Psychology and Center for Brain Science, Harvard University 52 Oxford Street, Room 290
Cambridge, MA 02138 USA

Correspondence should be addressed to Catherine Insel, Room 290, 52 Oxford Street, Cambridge, MA 02138 USA. E-mail: insel@fas.harvard.edu.

Abstract

Adolescence has been characterized as a developmental period of heightened reward seeking and attenuated aversive processing. However, it remains unclear how the neural bases of distinct outcome valuation processes shift during this stage of the lifespan. A total of 74 participants ranging in age from 13 to 20 years completed a value-modulated functional magnetic resonance imaging (fMRI) task in which participants earn low and high magnitude monetary outcomes to test whether gain and loss magnitude tracking—the neural representation of relative value in context—change differentially over this age span. Results revealed that gain and loss magnitude tracking follow asymmetric developmental trajectories. Gain magnitude tracking is elevated in the striatum during early adolescence and then decreases with age. By contrast, loss magnitude tracking in the anterior insula follows a quadratic pattern, undergoing a temporary attenuation during mid–late adolescence. A typical comparison of gain vs loss outcomes (collapsing over magnitude effects) showed robust activity across a suite of brain regions sensitive to value based on prior work including the ventral striatum, but they exhibited no changes with age. These findings suggest that value coding subprocesses follow divergent developmental paths across adolescence, which may contribute to normative shifts in adolescent motivated behavior.

Key words: adolescence; value; reward; loss; striatum; insula

Adolescence is a developmental window characterized by normative changes in motivated behavior. Research using animal models, human behavioral research and brain imaging work have broadly implicated a remodeling of behaviors and neurobiological signals relevant to valuation and motivation during adolescence (Somerville & Casey, 2010; Somerville et al., 2010; Hartley & Somerville, 2015). For example, adolescents are thought to exhibit heightened approach-related behavior toward rewards and attenuated processing of aversive cues (Doremus-Fitzwater & Spear, 2016). While most prior human neuroimaging research in this area has focused on reactivity to rewarding outcomes, valuation of outcome-related processes extends beyond mere reward reactivity. The present study quantifies a broadened

spectrum of neural signals contributing to gain and loss outcome value processing to chart developmental shifts in valuation relevant processing with greater specificity.

Human neuroimaging studies have identified the neural signals associated with gain and loss processing in adults (Delgado, 2007), which provide a framework to consider the development of valuation coding in the brain. Converging evidence has demonstrated that a distributed brain system codes the relative value of gain and loss outcomes (Bartra et al., 2013). The striatum and anterior insula represent key nodes within this valuation system (Knutson et al., 2014). Striatal activity increases with reward magnitude and promotes approach behavior (O'Doherty, 2004), whereas anterior insula

Received: 17 December 2017; **Revised:** 12 June 2018; **Accepted:** 11 July 2018

© The Author(s) (2018). Published by Oxford University Press.

This is an Open Access article distributed under the terms of the Creative Commons Attribution Non-Commercial License (<http://creativecommons.org/licenses/by-nc/4.0/>), which permits non-commercial re-use, distribution, and reproduction in any medium, provided the original work is properly cited. For commercial re-use, please contact journals.permissions@oup.com

activity tracks increasing loss magnitude (Samanez-Larkin et al., 2008) and enhances avoidance behavior (Palminteri et al., 2012). This form of value coding, which we will refer to as magnitude tracking, represents the span of value within a given context (Seymour & McClure, 2008) with parametrically increased neural activity during outcome receipt reflecting increasing context-relative value. Thus, the neural signals of these brain regions do not simply represent the presence of gain or loss but the relative magnitude of a given outcome compared to available alternatives. While gain and loss magnitude tracking has been well established in adults (Rangel & Clithero, 2012), it remains unknown whether this form of value signaling changes across development.

Prior work suggests that adolescents exhibit elevated reward reactivity in the striatum relative to younger and older ages (Galvan, 2010; Silverman et al., 2015). Reward reactivity is typically measured by comparing gain to loss outcomes or to baseline and in tasks that do not include magnitude manipulations (Ernst et al., 2005; van Leijenhorst et al., 2010; Op de Macks et al., 2011; van Duijvenvoorde et al., 2014) or collapse analyses across levels of value magnitude (van Leijenhorst et al., 2006; Braams et al., 2015). As a result, the developmental trajectory of outcome magnitude tracking remains largely unexplored. Additionally, few studies have examined the development of loss processing independent of reward outcomes. Prior work employing risky decision tasks have focused on neural responses during choice, which involved assessing potential reward and loss information simultaneously (Barkley-Levenson & Galvan, 2014; Barkley-Levenson et al., 2013; van Duijvenvoorde et al., 2015), making it difficult to parse the distinct mechanisms of appetitive and aversive processes. Further, these prior studies focused on decision value at the time of choice, and thus the developmental trajectories of gain and loss outcome processing remain unclear. The current study focused on incentive outcome processes to isolate developmental changes in neural processes that support magnitude tracking for gain and loss processes from conventional comparisons of reward reactivity.

In this study, participants completed a magnitude tracking task while undergoing functional magnetic resonance imaging. The task implemented a stakes manipulation, enabling independent measurement of neural responses to low and high magnitude gain and loss outcomes. In addition, the present study quantified the conventional gain vs loss processing comparison examined in prior work. We also conducted ancillary analyses to address the possibility that any observed age differences could be a byproduct of age-covarying factors such as fMRI data quality or differences in hedonic experience receiving the monetary incentives. By querying these related, but distinct, neural processes, we can gain a clearer picture of how development shapes neural valuation processes for gain and loss outcomes.

Materials and methods

Participants

A total of 79 participants between the ages of 13 and 20 years took part in this experiment. A total of 74 (38 females; M age = 17.22 years, $s.d.$ age = 2.31 years) participants were included in analyses, and five participants were excluded because of excessive in-scanner motion. The proportion of male and female participants did not significantly vary over the age range ($\chi^2(3) = 0.95$, $P = 0.81$; 13–14 years, 9 males and 8 females; 15–16 years, 7 males and 11 females; 17–18 years, 10 males and 9 females; 19–20 years, 10 males and 10 females). Participants

were screened for past or current psychiatric or neurological illness and had no lifetime use of psychotropic medication. Participants completed the Similarities and Matrix Reasoning sections of the Wechsler Abbreviated Scale of Intelligence (Wechsler, 2011). Full-scale intelligence quotient (IQ) was approximated using the age and sex specific t-score conversion (estimated IQ was unavailable for $n = 3$ participants). Estimated IQ did not vary across the age range, as there was no significant association between IQ and age ($r(69) = 0.082$, $P = 0.50$). The sample included left-handed ($n = 6$) and right-handed ($n = 66$) individuals, and handedness did not significantly vary by age ($\chi^2(3) = 3.796$, $P = 0.28$). Before study participation, participants and their legal guardians provided written assent and consent under the protocol approved by the Committee for Use of Human Subjects at Harvard University.

Magnitude tracking task

During functional neuroimaging, participants performed a task in which they received low-magnitude and high-magnitude gain and loss outcomes (Figure 1). This task was based on prior work (Delgado et al., 2000; Delgado et al. 2003) with the addition of a magnitude manipulation to compare responses to gains and losses at two levels of magnitude. First, participants viewed a low-stakes (+20¢/–10¢) or high-stakes (+\$1/–50¢) cue indicating the value of the upcoming four trials. On each trial, participants viewed a card turned over with a '?' and were instructed there was a number on the other side of the card between one and nine (but not five). Participants were instructed to press one of two buttons, indicating their guess of whether the number was lower than five (index finger) or higher than five (middle finger). Next, experimentally fixed feedback was displayed indicating whether they were correct (resulting in a monetary gain) or incorrect (resulting in a monetary loss).

In the high-stakes condition, correct feedback yielded a high-magnitude gain of \$1.00 and incorrect feedback and missed responses incurred a high-magnitude loss of 50¢. In the low-stakes condition, correct feedback yielded a low-magnitude gain of 20¢ and incorrect feedback and missed responses incurred a low-magnitude loss of 10¢. In total, 50% of trials delivered correct feedback with gain outcomes. The magnitude of the gain and loss incentives were chosen to allow for payout of all trials while also including a large number of trials for each condition, which ensured stable estimation of task conditions for the fMRI models. Participants were instructed that earnings would be paid out in full; however, all participants received \$15 as bonus payment at the end of the study, which was equivalent to the amount a participant could earn if no missed responses occurred. Number of missed responses did not vary by age (average response rate = 94.95%, correlation with age: $r(72) = 0.037$, $P = 0.76$).

The task was presented using PsychoPy software version 1.80 (Peirce, 2007) and displayed on a screen visible through a mirror attached to the head coil. Behavioral responses were collected with an MRI-compatible button box, and all participants used the index and middle finger of their dominant hand to make responses. Gain and loss feedback was pre-determined to include 50% correct (win) outcomes, and feedback presentation was pseudo-randomized within a block and ranged from one to three correct trials per block. Square frames surrounding trial stimuli (one-line frame for low-stakes and two-line frame for high-stakes) differentiated task from rest and provided a constant reminder of stakes conditions to reduce working memory demands.



Fig. 1. Magnitude tracking task. Participants viewed a cue (question mark) indicating they should guess whether the overturned card is greater or less than 5. Participants then received experimentally fixed feedback. The low-stakes block (top) delivers small gains and losses, whereas the high-stakes block (bottom) delivers large gains and losses. Each set of four trials is preceded by a cue indicating a forthcoming series of high or low stakes payout trials. This design permits separate comparison of neural response to receipt of gains vs losses (collapsed over stakes), magnitude tracking activity to high vs low gain outcomes and magnitude tracking of high vs low loss outcomes.

The task consisted of 24 blocks, which were presented across two functional runs lasting 422 s each. The order of low- and high-stakes blocks was pseudo-randomized within and across runs. Stakes cues were presented for 1 s, guess trials for 1.5 s and feedback/outcome for 1 s. Each block included one cue followed by four guess trials and four feedback/outcome displays. All task events were temporally separated by jittered interstimulus intervals ranging from 1.5 to 3.5 s and 8 s of fixation separated each block. In total, the task included 24 stakes cues (12 high-stakes/12 low-stakes), 96 guess trials (48 high/48 low), and 96 feedback events (24 high win +\$1.00, 24 high loss −\$0.50, 24 low win +\$0.20, 24 low loss −\$0.10).

fMRI acquisition and data processing

Participants were scanned on a Siemens 3.0 T Tim Trio scanner with a 32-channel head coil. Anatomical data were acquired with a high-resolution, T1-weighted anatomical scan using a multi-echo multiplanar rapidly acquired gradient-echo sequence (repetition time = 2530 ms, echo time = 1.74, 3.59, 5.44 and 7.29 ms, flip angle = 7°, field of view = 212 mm, slice thickness = 1 mm, voxel size = 1 × 1 × 1 mm) that is robust to head motion (Tisdall et al., 2012). fMRI blood-oxygen level dependent (BOLD) activity was measured over two functional runs. Functional data were acquired with a T2*-weighted echo-planar imaging (EPI) sequence with the following parameters: repetition time = 2 s, echo time = 30 ms, field of view = 216 mm, flip angle = 90°, voxel size = 3 × 3 × 3 mm. Thirty-one slices aligned to the anterior to posterior commissure plane were acquired per repetition time (TR), with a slice thickness of 3.75 mm. Prospective acquisition correction for head motion (Thesen et al., 2000) was implemented during functional scans to reduce motion-induced corruption of signal.

fMRI data processing and analysis were conducted with FMRIB Software Library (FSL) (version 5.0.4) (Smith et al., 2004). Pre-processing was conducted in FSL and implemented through the Lyman pipeline (v.0.0.7, <https://github.com/mwaskom>), which relies on the Nipype project framework (v.0.9.2) (Gorgolewski et al., 2011). Standard pre-processing steps included slice-time correction, realignment, coregistration of functional

to structural images using *bbregister* (Greve & Fischl, 2009), non-linear normalization of structural to FSL's MNI152 template space using *ANTS* 1.9.x, svn release 891; (Avants et al., 2009) and spatial smoothing with a 6 mm Gaussian kernel.

fMRI data were carefully evaluated for motion and signal outliers given the negative impact it can have on signal quality and general linear model (GLM) estimates. Five participants were excluded from analysis because of motion or data quality. The following rules were imposed for exclusion of functional data. Runs in which more than 10% of TRs were censored for motion (relative motion > 1 mm) or outlier signal intensity (exceeded the grand run median by 4.5 median absolute deviations) were excluded from analysis. Runs with a single relative movement exceeding 5 mm were also excluded. Participants with one usable run ($n = 4$) were included in analysis. In total, five participants were completely excluded for excessive motion (average age of excluded participants was 16.57 years; range, 14.24–17.71 years). In the full inclusion sample, there was no relationship between age and percent of censored data as measured by proportion of volumes excluded from analysis ($r(72) = -0.068$, $P = 0.56$).

Self-reported ratings

In a post-test, participants provided self-reported valence and arousal ratings for the task stimuli and monetary outcomes to assess for potential, co-occurring age differences in the hedonic experience of receiving the specific amounts of money used in the task. Ratings were collected using the Self-Assessment Manikin scales for valence and arousal (Lang, 1980). Valence ratings were given on a scale from 1 (unpleasant) to 9 (pleasant). Arousal ratings were scored on a scale from 1 (low arousal) to 9 (high arousal).

Analyses for the stimuli and hedonic experience ratings were implemented with linear mixed effects models using the *nlme* package in R (Pinheiro et al., 2014) and included factors for magnitude (high/low) and valence (gain/loss). Models for arousal and valence ratings were conducted separately. Models included self-reported rating as the dependent variable, magnitude (high/low) and valence (gain/loss) as fixed effects and subject as a random effect. To evaluate whether hedonic experience ratings were

consistent with age, linear and non-linear predictors of age were fit using the poly function and added as predictors to each model. A linear age predictor identified differences that increased or decreased with age, whereas a quadratic age predictor identified trajectories that peaked (inverted-U shape) or troughed (U-shape) during adolescence. The quadratic age predictor peaked at 17.22 years in this sample, very similar to the peak age of reward reactivity (gain vs loss contrast) reported in Braams et al. (2015). Model fits for linear and quadratic age predictors were compared using the analysis of variance function in R to determine whether the added age terms improved model fit. Together, these analyses isolated effects of valence (gain/loss), magnitude (high/low), their interaction and interactions with age on hedonic experience.

fMRI analysis

Pre-processed BOLD data were submitted to a GLM analysis using `film_gls` in FSL (Smith et al., 2004) to estimate relevant task effects. Regressors of interest included temporal onsets for the following task events: low-stakes cues, high-stakes cues, low-magnitude gains, high-magnitude gains, low-magnitude losses and high-magnitude losses. Additional regressors of non-interest modeled the choice period of trials with a single regressor modeling all guesses, and a second regressor modeling all missed responses. All task regressors were convolved with the canonical hemodynamic response function. Nuisance regressors included six-parameter motion correction and censored frames for deviant signal intensity and excessive motion. This model achieved uniformly low collinearity across regressors of interest (range: $r = -0.19$ – 0.21).

Random-effects group analyses (whole-brain voxelwise *t*-tests) were conducted to identify task-based changes in functional activity. The design of the task allowed for separate quantification of gain and loss magnitude tracking responses. Gain magnitude tracking was measured by comparing functional activity to high-magnitude vs low-magnitude rewards ($+\$1 > +20\text{¢}$). Loss magnitude tracking was measured by comparing functional activity to high-magnitude vs low-magnitude losses ($-50\text{¢} > -10\text{¢}$). Reward reactivity was measured by comparing all gains to all losses, collapsing over magnitude ($[\$1 + 20\text{¢}] > [-50\text{¢} - 10\text{¢}]$).

For these contrasts of interest, we first conducted analyses to identify neural regions responsive to gain and loss magnitude tracking in the whole sample, using one-sample *t*-tests. To assess age-related differences in brain activity for gain and loss magnitude tracking, mean-centered linear and quadratic age regressors were entered as covariates in the whole brain analyses just described. Whole brain maps were thresholded using whole-brain correction of $z > 2.3$ using FLAME 1 + 2, as implemented in FSL, resulting in whole-brain threshold of $P < 0.05$ family-wise error (FWE) corrected. Analyses implementing an initial threshold of $z > 2.3$ identified several large clusters spanning across many anatomical regions. Therefore, to better isolate distinct regions and delineate anatomical boundaries, we re-ran group analyses using a more stringent initial threshold of $z > 3$ before submitting maps to whole brain correction (FWE $P < 0.05$). Results from both analyses are reported in the cluster tables.

Significant age effects identified in the activation maps were supplemented with descriptive plotting of neural response by age to visualize the directionality of effects. To do so, we extracted parameter estimates from the activation loci using a 6 mm sphere around the peak activated voxel for cortical

regions or the full activated cluster for subcortical regions. Upon examining the linear age fit for the gain magnitude tracking (high > low reward) contrast, a notable outlier was detected that facilitated the statistical significance of the results. We verified that this participant was a highly influential data point based on a Cook's distance value that was three times greater than the mean distance (Stevens, 1984), which raised concern that the single data point may have skewed the results in a way that was not representative of the age-related trend. Therefore, we re-computed the statistical activation maps after removing this outlier (new analysis sample size, $n = 73$), and the results reported for this analysis reflect the smaller sample size.

Post-hoc exploratory analyses were performed using small volume correction (SVC) to further interrogate potential developmental trends that did not survive whole brain correction. The striatum was selected as a region of interest for these post-hoc exploratory analyses given that the striatum serves a key role in valuation signaling (Delgado, 2007; Liu et al., 2011; Barra et al., 2013), and adolescence has been previously characterized by increased striatal activity during reward outcome processing (Braams et al., 2015; Silverman et al., 2015). We generated an anatomically defined striatum mask consisting of the bilateral caudate, putamen and nucleus accumbens masks from the Harvard-Oxford atlas, thresholded at 10% probability (Desikan et al., 2006). We then queried for activations within this mask using SVC thresholding by implementing threshold-free cluster enhancement (TFCE) through the `randomize` function in FSL (Smith & Nichols, 2009), a conservative thresholding approach that eliminates the need to set an arbitrary threshold for initial cluster formation. TFCE was conducted with 5000 permutations, resulting in small volume threshold of $P < 0.05$ FWE corrected.

Cluster peaks are reported in cluster tables for the whole brain corrected maps reflecting an FWE $P < 0.05$ corrected threshold. Region labels are based on the Harvard-Oxford Cortical and Subcortical Atlases. Sub-clusters were defined by local maxima (activation peaks) within each cluster using a higher-values-first watershed searching algorithm, implemented in the Lyman pipeline (<https://github.com/mwaskom>).

Results

Loss magnitude tracking

Whole-brain analyses in the full sample identified a set of brain regions that exhibited enhanced recruitment for high-magnitude relative to low-magnitude losses ($-50\text{¢} > -10\text{¢}$ contrast). Results revealed that participants exhibited loss magnitude tracking in the right insula, right frontal pole, right middle frontal gyrus, bilateral cingulate and bilateral thalamus (Figure 2a, Table 1a).

Next, whole-brain linear and quadratic age analyses were computed to identify age-modulated loss magnitude tracking activity. No regions' activity surpassed whole brain correction for linear age or for the quadratic inverted-U model. For the quadratic age U-shaped model that troughed in mid-adolescence, we observed significant activity in the right anterior insula (1118 voxels at $X = 42$, $Y = 12$, $Z = 6$) extending into the operculum, right precentral gyrus and right middle frontal gyrus (Figure 2b and Table 1b). Descriptive plotting of the age interaction in the anterior insula confirmed that differential activity for high > low magnitude losses was highest in the youngest and oldest participants,

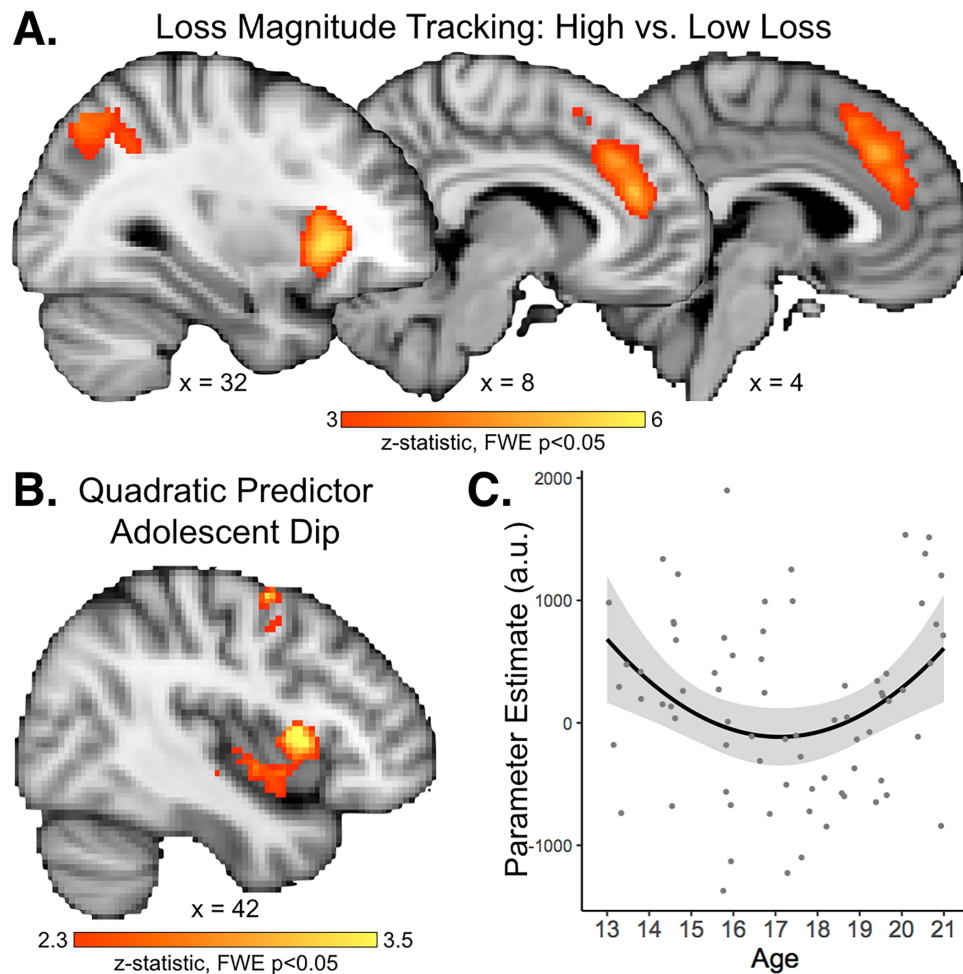


Fig. 2 . (A) Whole-brain analysis identifying neural regions exhibiting loss magnitude tracking (e.g. greater response to high than low value losses) in the full sample. (B) Neural regions demonstrating age-related change following a quadratic pattern. (C) Parameter estimates from right insula (Figure 2B) for high loss greater than low loss contrast reveals attenuation of loss magnitude tracking in adolescence. This plot is shown for descriptive purposes only.

and attenuated during mid-late adolescence (Figure 2c for visualization purposes).

Gain magnitude tracking

To measure gain magnitude tracking, whole-brain analyses identified regions exhibiting enhanced recruitment for high-magnitude relative to low-magnitude gains ($+\$1 > +\0.20). Gain magnitude tracking was associated with recruitment in the bilateral ventral striatum (nucleus accumbens) and dorsal striatum (caudate) extending into the thalamus, insula, frontal pole, cingulate, precuneus and precentral gyrus (Figure 3a and Table 2).

For the age covariate analyses, no regions survived whole-brain thresholding for either linear or quadratic age predictors. Given hypotheses regarding the role of the striatum in reward valuation, additional exploratory analyses were conducted within a striatum mask (containing the caudate, putamen and nucleus accumbens) with small volume correction (see Materials and methods for correction and outlier detection information). The linear age analysis revealed that within the striatum, there was greater gain magnitude tracking (i.e. differential recruitment for high relative to low magnitude rewards) in younger participants that decreased with increasing age in a

circumscribed region within right caudate (17 voxels at X = 10, Y = 24, Z = -2; Figure 3B and c, for visualization purposes only).

Reward reactivity

Similar to existing work, reward reactivity was measured by comparing activity that increased for gains relative to losses ($[\$1 > \$0.20] > [-\$0.20 & -\$0.10]$). This comparison was associated with enhanced recruitment of the ventral striatum (nucleus accumbens), dorsal striatum (caudate and putamen), cingulate, orbitofrontal cortex and precuneus (Figure 4A and Table 3). No regions survived whole-brain corrected thresholds in contrasts targeting age-related changes in gain vs loss activity following the linear or quadratic age patterns.

Although we did not observe any differential age-related responses to gain vs loss in whole brain analyses, we followed up with an exploratory region of interest (ROI) analysis focused on the striatum to query for even subtle effects, given prior work suggesting that reward reactivity peaks in mid-late adolescence (Braams et al., 2015). We used a watershed technique to identify the sub-peak activations within the boundaries of the left and right ventral striatum in the gain > loss analysis. We then extracted parameter estimates from these regions

Table 1. Regions exhibiting increased activity for loss magnitude tracking

Table 1.1: Loss magnitude tracking

High > low loss outcome #					
Region	z-stat	x	y	z	Voxels
Paracingulate gyrus	5.3	8	40	20	1057
Paracingulate gyrus	4.76	2	22	46	
Intracalcarine cortex	4.9	10	-84	6	828
Cerebellum	3.83	-34	-68	-50	
Insular cortex	5.8	32	22	0	682
Middle frontal gyrus	4.64	48	32	32	
Frontal pole	4.25	28	52	-4	
Superior frontal gyrus	3.58	26	8	54	
Lateral occipital cortex	4.42	30	-72	46	644
Supramarginal gyrus	3.27	50	-40	50	
Cerebellum	5.34	-10	-72	-28	538
Low > high loss outcome *					
Region	z-stat	x	y	z	Voxels
Precuneus cortex	6.49	-4	-56	24	11003
Postcentral gyrus	5.71	38	-24	54	
Postcentral gyrus	5.5	62	-8	36	
Lateral occipital cortex	5.17	-50	-72	24	1293
Central operculum cortex	5.15	-60	-18	12	3673
Planum temporale	5.17	62	-12	6	
Hippocampus	4.81	-28	-20	-14	580
Medial frontal cortex	4.25	-2	42	-14	447

Table 1.2: Loss magnitude tracking age analyses

High > Low Loss with linear increasing age * # : no regions**High > Low Loss with linear decreasing age * #** : no regions**High > Low Loss with quadratic \cap age * #** : no regions**High > Low Loss with quadratic U age #**

Region	z-stat	x	y	z	Voxels
Precentral gyrus	4.29	18	-30	64	1205
Supplementary motor cortex	3.67	-4	-4	70	
Middle frontal gyrus	3.55	38	0	60	
Insula/frontal operculum cortex	3.75	42	12	6	1118
Superior temporal gyrus	2.33	44	-20	-6	

Low > High Loss with linear increasing age * # : no regions**Low > High Loss with linear decreasing age * #** : no regions**Low > High Loss with quadratic \cap age * #** : no regions**Low > High Loss with quadratic U age * #** : no regions

Threshold $P < 0.05$ FWE corrected, with initial Z threshold of 3, denoted by *. For contrasts with no regions observed, the analysis was repeated with threshold of $P < 0.05$ FWE corrected, with initial Z threshold of 2.3, denoted by #.

(left: 22 voxels at $X = -12$, $Y = 8$, $Z = -6$; right: 18 voxels at $X = 12$, $Y = 10$, $Z = -4$) and plotted each ROI by age for visualization purposes. Visual inspection of both plots confirmed that there was no visible relationship with age (Figure 4B, right ventral striatum is depicted, although the left ventral striatum exhibits an equivalently flat age pattern).

Hedonic experience ratings

To verify that hedonic experience of the low and high magnitude gain and loss outcomes was consistent with age, participants provided self-reported valence (1 unpleasant to 9 pleasant) and arousal (1 low arousal to 9 high arousal) ratings for the task cues and incentive outcomes. For the cues, participants rated the cue denoting high-stakes as significantly more positive (high-stakes: $M = 5.89$, $s.d. = 1.26$; low-stakes: $M = 4.95$, $s.d. = 1.16$)

and more arousing (high-stakes: $M = 3.91$, $s.d. = 1.98$; low-stakes: $M = 2.45$, $s.d. = 1.62$) than low-stakes cues (see Table 5). Participants rated high-magnitude gains as significantly more positive (high gain: $M = 7.18$, $s.d. = 1.15$; low gain: $M = 6.23$, $s.d. = 0.90$) and arousing (high rewards: $M = 4.98$, $s.d. = 1.91$; low rewards: $M = 3.62$, $s.d. = 1.59$) than low-magnitude gains. Finally, participants rated high-magnitude losses as significantly more negative (high losses: $M = 2.37$, $s.d. = 1.19$; low losses: $M = 3.09$, $s.d. = 1.10$) and more arousing than low-magnitude losses (high losses: $M = 4.05$, $s.d. = 1.83$; low losses: $M = 2.70$, $s.d. = 1.66$). Valence and arousal ratings did not interact with linear or quadratic age trajectories for any of these classes of ratings. These analyses build confidence that the differences in gain and loss magnitude tracking cannot be explained by systematic age-related differences in hedonic experience when receiving money.

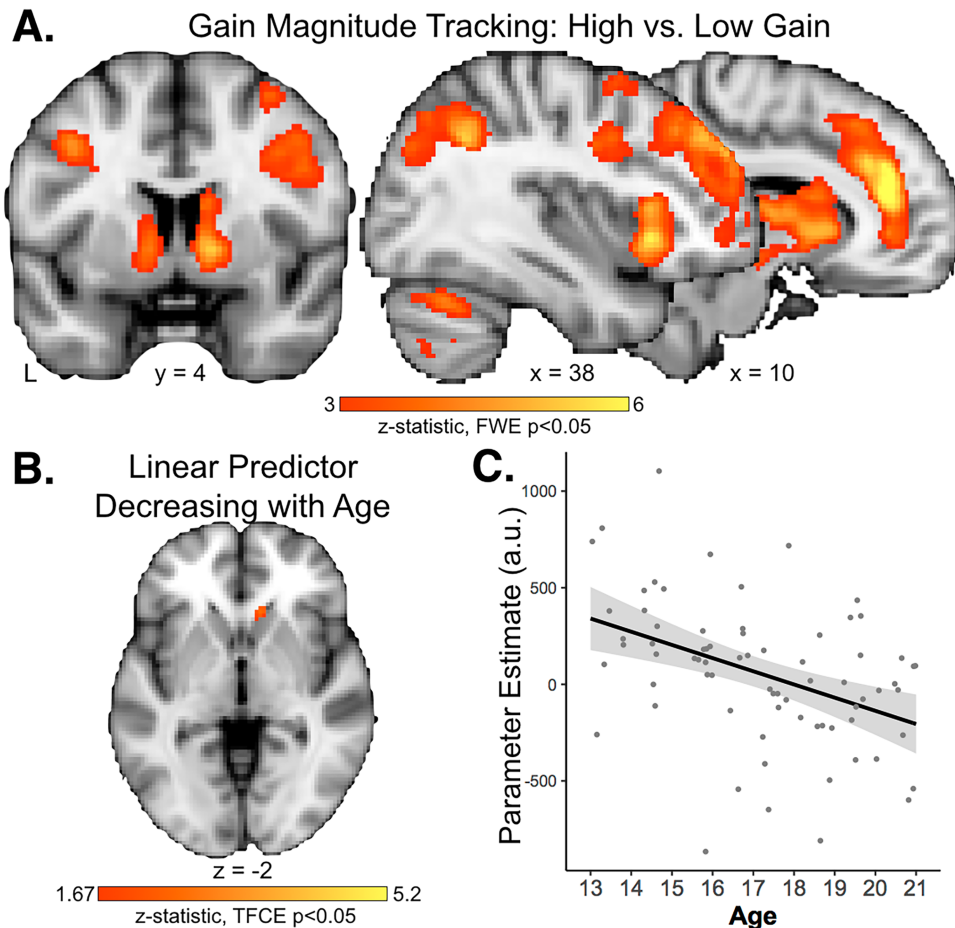


Figure 3. (A) Whole-brain analysis identifying neural regions exhibiting gain magnitude tracking (e.g. greater response to high than low value gains) in the full sample. (B) Neural regions demonstrating age-related change following a linear pattern, queried within a mask of the striatum ($P < 0.05$, TFCE small volume correction). (C) Parameter estimates from the caudate (Figure 3B) for high gain greater than low gain contrast reveals exaggerated gain magnitude tracking in early adolescence. This plot is shown for descriptive purposes only.

Discussion

The aim of this study was to identify how multiple neural valuation processes change across adolescence. During fMRI, we evaluated different facets of outcome valuation in adolescent and young adult participants aged 13 to 20 years by examining neural responses to gain and loss magnitude tracking in addition to analyses of reward reactivity. Results showed that distinct value representations followed asymmetric age-related change in patterns of neural recruitment within canonical valuation circuitry. Gain magnitude tracking decreased with age such that younger adolescents exhibited exaggerated magnitude tracking in the dorsal striatum for high relative to low gain outcomes compared to later ages. By contrast, loss magnitude tracking showed a quadratic effect of age in anterior insula response, with a significant drop during mid-adolescence. Reward reactivity analyses, which compared gain and loss outcomes while collapsing across low and high magnitudes, revealed no effect of age, suggesting that all ages increased striatal responses to gain relative to loss outcomes similarly. Together, these findings suggest that neurodevelopment exerts differential influence on distinct components of outcome valuation, which could be relevant to a variety of behavioral features that undergo normative change during this developmental window.

Magnitude tracking analyses isolated neural signals representing high-value relative to low-value outcomes. In the loss domain, across the group, a broad network of regions exhibited increased activation for high loss outcomes, including the insula, cingulate and thalamus. This pattern of recruitment converges with prior studies in adults examining the neural mechanisms supporting loss valuation (Bartra et al., 2013; Pessiglione & Delgado, 2015). Quadratic age analyses revealed that loss magnitude tracking was maximally attenuated during mid-adolescence in the anterior insula, suggesting that loss magnitude tracking may undergo a temporary period of attenuation during adolescence. Loss-related processing in the anterior insula has been linked to avoidance learning from punishments (Samanez-Larkin et al., 2008; Palminteri et al., 2012), suggesting that insula activity may subserve the ability to use negative outcomes to incrementally update value representations. Though future work is needed to elucidate the behavioral consequences of this trajectory, it stimulates hypotheses about whether attenuated loss value processing is a key mechanism that contributes to adolescents' tendency toward risky decision-making (Figner et al., 2009; Defoe et al., 2015; Powers et al., *in press*) and altered learning from or sensitivity to negative feedback (van Duijvenvoorde et al., 2008; van den Bos et al., 2012; Rodman et al., 2017).

Table 2. Regions exhibiting increased activity for gain magnitude tracking

Table 2.1: Gain magnitude tracking group map

High > low gain outcome *					
Region	z-stat	X	y	z	Voxels
Paracingulate gyrus	6.63	10	40	20	11389
Insular cortex	6.26	28	18	-8	
Frontal pole	5.66	40	40	36	
Thalamus	5.61	4	-12	10	
Superior frontal gyrus	5.46	4	26	48	
Frontal pole	4.81	20	54	-8	
Cerebellum	5.93	-24	-66	-30	5385
Occipital pole	5.16	-4	-96	0	
Cerebellum	4.54	36	-62	-28	
Angular gyrus	5.39	38	-54	36	1375
Insular cortex	5.8	-28	22	-6	648
Precentral gyrus	4.66	-36	0	38	474
Low > high gain outcome *					
Region	z-stat	X	y	z	Voxels
Postcentral gyrus	5.15	12	-36	54	3018
Supplementary motor area	4.7	-10	-14	50	
Precentral gyrus	4.62	60	2	10	
Central operculum cortex	5.41	-52	-4	8	2053
Parietal operculum cortex	5.38	44	-22	22	1457
Postcentral gyrus	4.24	-52	-22	42	388

Table 2.2: Gain magnitude tracking age analyses

High > low gain with linear increasing age * #: no regions
High > low gain with linear decreasing age * #: no regions
High > low gain with quadratic \cap age * #: no regions
High > low gain with quadratic U age * #: no regions
Low > high gain with linear increasing age * #: no regions
Low > high gain with linear decreasing age * #: no regions
Low > high gain with quadratic \cap age * #: no regions
Low > high gain with quadratic U age * #: no regions

Threshold $P < 0.05$ FWE corrected, with initial Z threshold of 3, denoted by *. For contrasts with no regions observed, the analysis was repeated with threshold of $P < 0.05$ FWE corrected, with initial Z threshold of 2.3, denoted by #.

Gain magnitude tracking analyses separately identified regions exhibiting enhanced activation for high relative to low value gain outcomes. Across the group, there was increased recruitment in the bilateral ventral striatum, caudate, thalamus, insula, cingulate and medial prefrontal cortex, a suite of brain regions commonly identified as a reward valuation network (Delgado, 2007; Haber & Knutson, 2010; Liu et al., 2011; Bartra et al., 2013). Age comparisons indicated that activity in these regions were largely consistent across age, converging with prior developmental work assessing high- compared to low-value outcomes (Insel et al., 2017). The sole exception was elevated gain magnitude tracking in the caudate in early adolescence that decreased progressively with increasing age.

Prior work suggests that adolescents exhibit heightened magnitude tracking in the ventral striatum compared to young adults when computing the expected value of a choice during risky decisions and also when passively receiving high- vs low-magnitude rewards (Galvan et al., 2006; Barkley-Levenson & Galvan, 2014). However, it is important to note that this prior work interrogated age differences using a ventral striatum ROI, rather than more broadly across the striatum or whole brain. Here we identified age-related changes in gain magnitude tracking in the dorsal striatum. Notably, research using a whole-brain analysis approach has demonstrated that in the context

of a reinforcement learning task, adolescents exhibit elevated reward prediction error coding in the dorsal striatum at the time of reward feedback (outcome stage) relative to children and adults (Cohen et al., 2010). The striatum is a heterogeneous region with diverse functional roles (Haber & Knutson, 2010), and therefore it will be important for future work to consider striatal 'hyperresponding' in adolescence with greater anatomical specificity. Moreover, the elevation in dorsal striatal response in young adolescents observed here did not survive whole-brain correction but was found in a very constrained cluster when implementing small-volume correction using a striatal mask. The current findings suggest that age-related gain magnitude tracking biases in the striatum are modest.

These age-related patterns of neural magnitude tracking were not confounded by age-related differences in hedonic experience for winning and losing money. If participants in a certain age range reported a greater or lesser hedonic response to money, this would present an interpretational confound for the observed age effects (Davidow et al., in press). We found no evidence for age-related differences in the relative valence or arousal of low and high gains or low and high losses. This builds confidence in interpreting these signal differences as age-related, rather than experiential.

Table 3. Regions exhibiting increased activity for gain vs loss reactivity

Table 3.1: Reward reactivity group map

Gain > loss *					
Region	z-stat	x	y	z	Voxels
Caudate	9.59	12	10	-4	98538
Cingulate gyrus	7.67	-4	-34	38	
Paracingulate gyrus	7.23	4	50	4	
Cerebellum	7.09	42	-66	-38	
Frontal orbital cortex	6.54	-26	34	-10	
Precentral gyrus	6.42	-14	-26	66	
Loss > gain * #: no regions					

Table 3.2: Reward reactivity age analyses

Gain > loss with linear increasing age * #: no regions
 Gain > loss with linear decreasing age * #: no regions
 Gain > loss with quadratic \cap age * #: no regions
 Gain > loss with quadratic \cup age * #: no regions
 Loss > gain with linear increasing age * #: no regions
 Loss > gain with linear decreasing age * #: no regions
 Loss > gain with quadratic \cap age * #: no regions
 Loss > gain with quadratic \cup age * #: no regions

Threshold $P < 0.05$ FWE corrected, with initial Z threshold of 3, denoted by *. For contrasts with no regions observed, the analysis was repeated with threshold of $P < 0.05$ FWE corrected, with initial Z threshold of 2.3, denoted by #.

Table 4. Hedonic Experience rating analysis

Stakes cues	Valence			Arousal		
	b	t	P	b	t	P
Magnitude	0.95	6.04	<0.0001	1.45	7.02	<0.0001
Linear age	1.63	0.95	0.34	-3.89	-1.52	0.13
Quadratic age	0.61	0.36	0.72	-2.93	-1.15	0.26
Magnitude * linear age	-0.72	-0.38	0.71	1.70	0.68	0.50
Magnitude* quadratic age	1.09	0.57	0.57	1.86	0.74	0.46
Gain outcomes	b	t	P	b	t	P
Magnitude	0.95	5.84	<0.0001	1.36	9.32	<0.0001
Linear age	0.87	0.59	0.55	-3.29	-1.33	0.19
Quadratic age	-1.72	-1.18	0.24	-2.32	-0.94	0.35
Magnitude * linear age	-1.94	-0.99	0.33	0.67	0.38	0.71
Magnitude * quadratic age	-0.45	-0.23	0.82	-0.71	-0.40	0.69
Loss outcomes	b	t	P	b	t	P
Magnitude	-0.72	-6.37	<0.0001	1.35	7.83	<0.0001
Linear age	3.83	2.41	0.02	-2.56	-1.03	0.31
Quadratic age	-0.01	-0.01	0.99	-2.05	-0.82	0.41
Magnitude * linear age	-0.50	-0.37	0.71	0.74	0.35	0.73
Magnitude * quadratic age	0.95	0.69	0.49	0.12	0.06	0.95

An open question is whether different developmental trends in magnitude tracking would emerge if even higher magnitude gains and losses were at stake. Converging evidence suggests that outcome value is represented in a relative fashion, and brain

activity tracks a relative difference from the potential best and worst options one could experience in a given context (Seymour & McClure, 2008). While this task compared gains of 20¢ and \$1, we believe that these effects would generalize to various

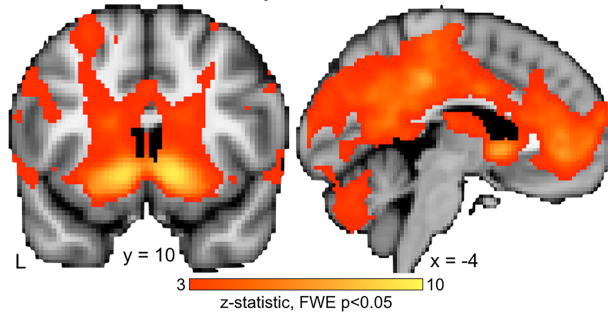
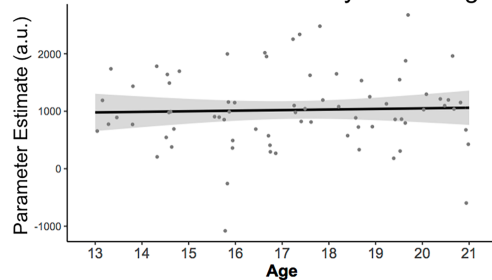
A. Reward Reactivity: Gain vs. Loss Outcome**B. Striatum Reward Reactivity across Age**

Figure 4. (A) Whole-brain analysis identifying neural regions exhibiting reward reactivity (e.g., greater response to gain than loss feedback) in the full sample. (B) Region of interest analysis confirming lack of age differences on the ventral striatum response to gain vs loss contrast. The right ventral striatum is depicted for visualization purposes, although the left ventral striatum is equivalently flat.

magnitudes with similar relative value in low- and high-stakes (e.g. \$1 vs \$5 or \$2 vs \$10). However, future work is needed to assess how larger ratios of high- to low-stakes incentives (e.g. 20¢ vs \$10) may impact developmental differences. Further, the developmental trajectories of outcome processing may differ from age-related differences in incentive anticipation or choice value computation. Future work should examine how these distinct subcomponents of valuation may vary across adolescence.

A key feature of the present design is the ability to separate the magnitude tracking responses just described from the more canonical assessments of reward reactivity that isolate neural signals with greater response to gains than losses. In the present study, reward reactivity was assessed by comparing gain to loss outcomes and collapsing across magnitude conditions. Across the sample, there was robust increased recruitment for gains in the ventral striatum, caudate, putamen, medial prefrontal cortex and posterior cingulate, converging with prior studies of adults examining the neural bases of reward processing (Delgado et al., 2000; Delgado, 2007).

Surprisingly, there was no effect of age on the reward reactivity response in any of these regions, even when specifically targeting the ventral striatum with constrained ROI analyses. This is inconsistent with prior developmental work suggesting that striatal reward reactivity peaks during mid-adolescence (Galvan, 2010; Braams et al., 2015; Silverman et al., 2015) and theoretical accounts proposing that adolescents are hypersensitive to rewards writ-large. While we found no effect of age on reward reactivity, this may potentially reflect a constrained age range, as other work has tested a wider developmental span extending earlier into childhood and later into young adulthood. For example, Braams et al. (2015) reported a peak in reward activity around age 17 years when testing a sample range of

8 to 27 years old. That said, this study joins several others in their failure to identify adolescent-elevated reward reactivity in the ventral striatum (May et al., 2004; Forbes et al., 2010). This could suggest that developmental trends in reward processing are subtler than previously appreciated (Sherman et al., 2017).

Our findings also suggest that attenuated sensitivity to loss magnitude could inadvertently influence statistical comparisons of gain vs loss where loss reflects the baseline condition, since reward valuation signals are largely considered to be coded in the brain relative to the dynamic range of outcome values available in a given environment (Seymour & McClure, 2008). Further, the current task is designed with higher magnitude gain than loss outcomes to mitigate the potential influence of prospect theory (e.g. the phenomenon that losses loom larger than gains, and therefore a loss of 50¢ may hold larger unsigned value than a gain of 50¢) (Kahneman & Tversky, 1979; Delgado, 2007). Therefore, each trial has a positive expected value in an absolute sense, even though reward and loss are believed to be more balanced in a subjective sense. However, in other reward reactivity tasks that do not follow the principles of prospect theory, losses could differentially ‘anchor’ value scaling responses and interact differently given mid-adolescents’ attenuation of loss scaling. These findings suggest that more work will be needed to characterize the specificity and boundaries of adolescent neural reward reactivity.

Together, these findings suggest that adolescence is characterized by a temporary attenuation in loss magnitude tracking and an early sensitization to gain magnitude tracking. The combination of these distinct trajectories may, in part, shape normative shifts in adolescent motivated behavior. The present results comport with converging animal studies, which have demonstrated that the adolescent stage is accompanied by reduced behavioral sensitization to punishment. For example, juvenile rodents experience attenuated responses to aversive stimuli, such as decreased sensitivity to the negative effects of alcohol exposure or drug-related withdrawal symptoms (Doremus-Fitzwater & Spear, 2016). Moreover, adolescent-stage rodents have difficulty learning from aversive feedback relative to younger and older ages, and this stage is accompanied by a temporary suppression of behavioral reactions to aversive contexts, which recovers in early adulthood (Pattwell et al., 2011, 2012; 2016). The current loss magnitude tracking results converge with work in non-human animal models of development and provide evidence for the human neurodevelopmental changes that support attenuated aversive processing, which could result in reduced avoidance behavior during this period of the lifespan. This work highlights attenuated loss processing as a key facet of adolescent motivational change.

In sum, the present study revealed asymmetric neurodevelopmental shifts in distinct outcome valuation processes. This study employed an experimental paradigm capable of separately isolating changes in gain vs loss processing (reward reactivity), gain magnitude tracking and loss magnitude tracking in a sample of healthy 13–20-year-olds. Results indicated that loss magnitude tracking in the insula exhibits a temporary decrease in mid-adolescence while gain magnitude tracking in the striatum is heightened in early stages but then declines with age. More generally, this work demonstrates that the manner in which valuation-related processes is queried exerts a strong influence on the developmental profiles observed, guiding future work toward charting the development of valuation processes with greater specificity. Future work should investigate how asymmetric gain and loss valuation trajectories influence motivated goal directed behavior.

Funding

This research was supported in part by the National Science Foundation (Graduate Research Fellowship DGE 1144152 to C.I.; CAREER grant BCS 1452530 to L.H.S.), the Sackler Scholar Programme in Psychobiology (to C.I.) and the FJ McGuigan Young Investigator Prize for Understanding the Human Mind (to L.H.S.).

Acknowledgements

We thank Chiemeka Ezie, Megan Garrad, Catherine Glenn, Eliza Lanzillo, Kristen Osborne, Stephanie Sasse, and Constanza Vidal Bustamante for assistance with recruitment and testing.

References

- Avants, B.B., Tustison, N., Song, G. (2009). Advanced normalization tools (ANTS). *The Insight Journal*, 2, 1–35.
- Barkley-Levenson, E., Galvan, A. (2014). Neural representation of expected value in the adolescent brain. *Proceedings of the National Academy of Sciences of the United States of America*, 111(4), 1646–51.
- Barkley-Levenson, E., van Leijenhorst, L., Galvan, A. (2013). Behavioral and neural correlates of loss aversion and risk avoidance in adolescents and adults. *Developmental cognitive neuroscience*, 3, 72–83.
- Bartra, O., McGuire, J.T., Kable, J.W. (2013). The valuation system: a coordinate-based meta-analysis of BOLD fMRI experiments examining neural correlates of subjective value. *Neuroimage*, 76, 412–27.
- Braams, B.R., van Duijvenvoorde, A.C., Peper, J.S., Crone, E.A. (2015). Longitudinal changes in adolescent risk-taking: a comprehensive study of neural responses to rewards, pubertal development, and risk-taking behavior. *The Journal of Neuroscience: the Official Journal of the Society for Neuroscience*, 35(18), 7226–7238.
- Cohen, J.R., Asarnow, R.F., Sabb, F.W., et al. (2010). A unique adolescent response to reward prediction errors. *Nature Neuroscience*, 13(6), 669–71.
- Davidow, J.Y., Insel, C., Somerville, L.H. (2018). Adolescent development of value-guided goal pursuit. *Trends in Cognitive Sciences*, 22(8), 725–36.
- Defoe, I.N., Dubas, J.S., Figner, B., van Aken, M.A. (2015). A meta-analysis on age differences in risky decision making: adolescents versus children and adults. *Psychological Bulletin*, 141(1), 48–84.
- Delgado, M.R. (2007). Reward-related responses in the human striatum. *Annals of the New York Academy of Sciences*, 1104, 70–88.
- Delgado, M.R., Locke, H.M., Stenger, V.A., Fiez, J.A., Fiez, J.A. (2003). Dorsal striatum responses to reward and punishment: effects of valence and magnitude manipulations. *Cognitive, Affective, & Behavioral Neuroscience*, 3(1), 27–38.
- Delgado, M.R., Nystrom, L.E., Fissell, C., Noll, D.C., Fiez, J.A. (2000). Tracking the hemodynamic responses to reward and punishment in the striatum. *Journal of Neurophysiology*, 84(6), 3072–7.
- Desikan, R.S., Segonne, F., Fischl, B., et al. (2006). An automated labeling system for subdividing the human cerebral cortex on MRI scans into gyral based regions of interest. *Neuroimage*, 31(3), 968–80.
- Doremus-Fitzwater, T.L., Spear, L.P. (2016). Reward-centricity and attenuated aversions: An adolescent phenotype emerging from studies in laboratory animals. *Neuroscience and Biobehavioral Reviews*, 70, 121–34.
- Ernst, M., Nelson, E.E., Jazbec, S., et al. (2005). Amygdala and nucleus accumbens in responses to receipt and omission of gains in adults and adolescents. *Neuroimage*, 25(4), 1279–91.
- Figner, B., Mackinlay, R.J., Wilkening, F., Weber, E.U. (2009). Affective and deliberative processes in risky choice: age differences in risk taking in the Columbia Card Task. *Journal of Experimental Psychology: Learning, Memory, and Cognition*, 35(3), 709–30.
- Forbes, E.E., Ryan, N.D., Phillips, M.L., et al. (2010). Healthy adolescents' neural response to reward: associations with puberty, positive affect, and depressive symptoms. *Journal of the American Academy of Child and Adolescent Psychiatry*, 49(2), 162–72 e161–e165.
- Galvan, A. (2010). Adolescent development of the reward system. *Frontiers in Human Neuroscience*, 4, 6.
- Galvan, A., Hare, T.A., Parra, C.E., et al. (2006). Earlier development of the accumbens relative to orbitofrontal cortex might underlie risk-taking behavior in adolescents. *The Journal of Neuroscience*, 26(25), 6885–92.
- Gorgolewski, K., Burns, C.D., Madison, C., et al. (2011). Nipype: a flexible, lightweight and extensible neuroimaging data processing framework in python. *Frontiers in Neuroinformatics*, 5, 13.
- Greve, D.N., Fischl, B. (2009). Accurate and robust brain image alignment using boundary-based registration. *Neuroimage*, 48(1), 63–72.
- Haber, S.N., Knutson, B. (2010). The reward circuit: linking primate anatomy and human imaging. *Neuropsychopharmacology*, 35(1), 4–26.
- Hartley, C.A., Somerville, L.H. (2015). The neuroscience of adolescent decision-making. *Current Opinion in Behavioral Sciences*, 5, 108–15.
- Insel, C., Kastman, E.K., Glenn, C.R., Somerville, L.H. (2017). Development of corticostriatal connectivity constrains goal-directed behavior during adolescence. *Nature Communications*, 8(1), 1605.
- Kahneman, D., Tversky, A. (1979). Prospect theory: an analysis of decision under risk. *Econometrica*, 47(2), 263–92.
- Knutson, B., Katovich, K., Suri, G. (2014). Inferring affect from fMRI data. *Trends in Cognitive Sciences*, 18(8), 422–8.
- Lang, P.J. (1980). *Self-Assessment Manikin*, Gainesville, FL: The Center for Research in Psychophysiology, University of Florida.
- Liu, X., Hairston, J., Schrier, M., Fan, J. (2011). Common and distinct networks underlying reward valence and processing stages: a meta-analysis of functional neuroimaging studies. *Neuroscience & Biobehavioral Reviews*, 35(5), 1219–36.
- May, J.C., Delgado, M.R., Dahl, R.E., et al. (2004). Event-related functional magnetic resonance imaging of reward-related brain circuitry in children and adolescents. *Biological Psychiatry*, 55(4), 359–66.
- O'Doherty, J.P. (2004). Reward representations and reward-related learning in the human brain: insights from neuroimaging. *Current Opinion in Neurology*, 14(6), 769–76.
- Op de Macks, Z.A., Gunther Moor, B., Overgaauw, S., Guroglu, B., Dahl, R.E., Crone, E.A. (2011). Testosterone levels correspond with increased ventral striatum activation in response to monetary rewards in adolescents. *Developmental Cognitive Neuroscience*, 1(4), 506–16.
- Palminteri, S., Justo, D., Jauffret, C., et al. (2012). Critical roles for anterior insula and dorsal striatum in punishment-based avoidance learning. *Neuron*, 76(5), 998–1009.
- Pattwell, S.S., Bath, K.G., Casey, B.J., Ninan, I., Lee, F.S. (2011). Selective early-acquired fear memories undergo temporary

- suppression during adolescence. *Proceedings of the National Academy of Sciences of the United States of America*, **108**(3), 1182–7.
- Pattwell, S.S., Duhoux, S., Hartley, C.A., et al. (2012). Altered fear learning across development in both mouse and human. *Proceedings of the National Academy of Sciences of the United States of America*, **109**(40), 16318–23.
- Pattwell, S.S., Liston, C., Jing, D., et al. (2016). Dynamic changes in neural circuitry during adolescence are associated with persistent attenuation of fear memories. *Nature Communications*, **7**, 11475.
- Pearce, J.W. (2007). PsychoPy—Psychophysics software in Python. *Journal of Neuroscience Methods*, **162**(1–2), 8–13.
- Pessiglione, M., Delgado, M.R. (2015). The good, the bad and the brain: neural correlates of appetitive and aversive values underlying decision making. *Current Opinion in Behavioral Sciences*, **5**, 78–84.
- Pinheiro, J., Bates, D., DebRoy, S., Sarkar, D., R Core Team. (2014). nlme: linear and nonlinear mixed effects models. Available at: <http://cran.r-project.org/package=nlme>.
- Powers, K.E., Yaffe, G., Hartley, C.A., Davidow, J.Y., Kober, H., Somerville, L.H. (2018). Consequences for peers differentially bias computations about risk from adolescence to adulthood. *Journal of Experimental Psychology: General*, **147**(5), 671–82.
- Rangel, A., Clithero, J.A. (2012). Value normalization in decision making: theory and evidence. *Current Opinion in Neurobiology*, **22**(6), 970–81.
- Rodman, A.M., Powers, K.E., Somerville, L.H. (2017). Development of self-protective biases in response to social evaluative feedback. *Proceedings of the National Academy of Sciences of the United States of America*, **114**(50), 13158–63.
- Samanez-Larkin, G.R., Hollon, N.G., Carstensen, L.L., Knutson, B. (2008). Individual differences in insular sensitivity during loss anticipation predict avoidance learning. *Psychological Science*, **19**(4), 320–3.
- Seymour, B., McClure, S.M. (2008). Anchors, scales and the relative coding of value in the brain. *Current Opinion in Neurobiology*, **18**(2), 173–8.
- Sherman, L., Steinberg, L., Chein, J. (2017). Connecting brain responsivity and real-world risk taking: Strengths and limitations of current methodological approaches. *Developmental Cognitive Neuroscience*.
- Silverman, M.H., Jedd, K., Luciana, M. (2015). Neural networks involved in adolescent reward processing: An activation likelihood estimation meta-analysis of functional neuroimaging studies. *Neuroimage*, **122**, 427–39.
- Smith, S.M., Jenkinson, M., Woolrich, M.W., et al. (2004). Advances in functional and structural MR image analysis and implementation as FSL. *Neuroimage*, **23**(Suppl 1), S208–19.
- Smith, S.M., Nichols, T.E. (2009). Threshold-free cluster enhancement: addressing problems of smoothing, threshold dependence and localisation in cluster inference. *Neuroimage*, **44**(1), 83–98.
- Somerville, L.H., Casey, B.J. (2010). Developmental neurobiology of cognitive control and motivational systems. *Current Opinion in Neurobiology*, **20**(2), 236–41.
- Somerville, L.H., Jones, R.M., Casey, B.J. (2010). A time of change: behavioral and neural correlates of adolescent sensitivity to appetitive and aversive environmental cues. *Brain and Cognition*, **72**(1), 124–33.
- Stevens, J.P. (1984). Outliers and influential data points in regression analysis. *Psychological Bulletin*, **95**(2), 334–44.
- Thesen, S., Heid, O., Mueller, E., Schad, L.R. (2000). Prospective acquisition correction for head motion with image-based tracking for real-time fMRI. *Magnetic Resonance in Medicine*, **44**(3), 457–65.
- Tisdall, M.D., Hess, A.T., Reuter, M., Meintjes, E.M., Fischl, B., van der Kouwe, A.J. (2012). Volumetric navigators for prospective motion correction and selective reacquisition in neuroanatomical MRI. *Magnetic Resonance in Medicine*, **68**(2), 389–399.
- van den Bos, W., Cohen, M.X., Kahnt, T., Crone, E.A. (2012). Striatum-medial prefrontal cortex connectivity predicts developmental changes in reinforcement learning. *Cerebral Cortex*, **22**(6), 1247–1255.
- van Duijvenvoorde, A.C., Huizenga, H.M., Somerville, L.H., et al. (2015). Neural correlates of expected risks and returns in risky choice across development. *The Journal of Neuroscience: the Official Journal of the Society for Neuroscience*, **35**(4), 1549–1560.
- van Duijvenvoorde, A.C., Op de Macks, Z.A., Overgaauw, S., Gunther Moor, B., Dahl, R.E., Crone, E.A. (2014). A cross-sectional and longitudinal analysis of reward-related brain activation: effects of age, pubertal stage, and reward sensitivity. *Brain and Cognition*, **89**, 3–14.
- van Duijvenvoorde, A.C., Zanolie, K., Rombouts, S.A., Raijmakers, M.E., Crone, E.A. (2008). Evaluating the negative or valuing the positive? Neural mechanisms supporting feedback-based learning across development. *The Journal of Neuroscience: the Official Journal of the Society for Neuroscience*, **28**(38), 9495–9503.
- van Leijenhorst, L., Crone, E.A., Bunge, S. A. (2006). Neural correlates of developmental differences in risk estimation and feedback processing. *Neuropsychologia*, **44**(11), 2158–2170.
- van Leijenhorst, L., Zanolie, K., Van Meel, C. S., Westenberg, P.M., Rombouts, S.A., Crone, E.A. (2010). What motivates the adolescent? Brain regions mediating reward sensitivity across adolescence. *Cerebral Cortex*, **20**(1), 61–69.
- Wechsler, D. (2011). WASI II: Wechsler Abbreviated Scale of Intelligence (2nd ed.): Psychological Corporation.